Effects of fishing on a protogynous hermaphrodite

Paul R. Armsworth

Abstract: Population dynamic models and simulations are analysed for a harvested reef fish species that is a monandric, protogynous hermaphrodite. The models are applied to data for the coral trout *Plectropomus leopardus* (Pisces: Serranidae) on the Great Barrier Reef. One model examines the situation where sexual transition is induced by some exogenous behavioural mechanism, and another considers the case where transition is determined by some endogenous developmental schedule. The conclusions regarding the effects of fishing are common to both models, and the implementation of more efficient harvesting practices may not require a precise understanding of the mechanisms governing sexual transition.

Résumé : On trouvera ici une analyse de modèles et de simulations de la dynamique d'une population de poissons de récif hermaphrodites monandres et protogynes qui est soumise à pêche commerciale. Les modèles ont été appliqués à des données provenant d'une population du serranidé, *Plectropomus leopardus* (Pisces: Serranidae), du récif de la Grande Barrière. L'un des modèles examine la situation où la transition sexuelle est causée par un mécanisme comportemental exogène et l'autre celle où cette transition est déterminé par un calendrier de développement endogène. Les effets de la pêche calculés à l'aide des deux modèles sont semblables; il n'est donc probablement pas nécessaire de connaître de façon précise les mécanismes qui régissent la transition sexuelle pour mettre en place des pratiques de pêche plus efficaces.

[Traduit par la Rédaction]

Introduction

Many commercially important reef fish species are hermaphrodites. Fisheries theory developed for gonochoristic populations may not be applicable to these species (Bannerot et al. 1987; Russ 1991). Models and simulations that examine the effects of harvesting on a hermaphroditic fish are presented and these are applied to data for the coral trout or leopard coral grouper *Plectropomus leopardus* (Pisces: Serranidae). Coral trout are sequential hermaphrodites, in which the hermaphroditism is protogynous (female–male) and monandric (males are only produced through sexual transition) (Thresher 1984; Ferreira 1995). The species is a long-lived, apex predator on the Great Barrier Reef. The burgeoning literature on *P. leopardus* serves as testament to its commercial importance in Australia. Coral trout comprise 30% of the total catch of the Queensland commercial line-fishing fleet, and the stocks support a booming, recreational line fishery (Ferreira and Russ 1994).

Two types of mechanism could induce sexual transition in hermaphroditic fishes. Either exogenous behavioural mechanisms could determine the timing of transition, such as the size of an individual relative to other members of its social group, or transition could be associated with some endogenous developmental schedule, such as absolute size or age. While exogenous mechanisms have been detected (Shapiro 1989; Ross 1990), endogenous mechanisms may still be important in some species (Thompson and Munro 1983; Buxton 1993) or may interact with exogenous factors. If fishing is size selective, then the consequences for population structure depend on mechanisms governing transition. If sex change is governed by social mechanisms, then transition would be expected to occur earlier in the life cycle when older, single-sex individuals are removed. This would cause the mean size and age of females to decrease for protogynous species and could cause a reduction in egg production. If sexual transition were driven by some fixed developmental schedule, the population could not compensate for impacts to its sex ratio. Selective fishing of older individuals would then lead to sex ratios that were shifted from their natural state; these would be female biased for protogynous hermaphrodites.

In the models and simulations, particular attention is paid to the importance of metapopulation concepts and fluctuating recruitment levels. As is conventional in reef fish ecology, "recruitment" refers here to recruitment to a local adult population following pelagic larval dispersal and does not refer to age of first vulnerability to gear. Harvesting causes a directional shift through parameter space. The consequences of fishing for population dynamics can be understood by examining the magnitude of the change in parameter values and comparing this with the deterministic and stochastic analyses. In the following section, the model formulation and the deterministic and stochastic dynamics are described. Then later, the effects of harvesting and the size of the movement through parameter space that results from fishing are considered.

P.R. Armsworth.[1] School of Mathematical and Physical Sciences, James Cook University, Townsville, Queensland 4811, Australia.

[1]Present address: Department of Biological Sciences, Stanford University, Stanford, CA 94305-5020, U.S.A. (e-mail: armsworth@stanford.edu).

Population model

The population is structured into ω age-classes, $\mathbf{N} = (N_1,...,N_\omega)$, with reproduction occurring in a short annual spawning season. This is representative of coral trout behaviour on the Great Barrier Reef (Doherty et al. 1994; Samoilys and Squire 1994). The census time is set immediately before reproduction.

Each year-class is subdivided by sex, with $f_i = f_i(\mathbf{N})$ and $m_i = m_i(\mathbf{N})$ denoting the expected proportion of the ith year-class that is female and male, respectively. As hermaphroditism is protogynous, $f_i > m_i$ for younger age-classes. In Model 1, sexual transition is governed by an endogenous developmental schedule, and an individual female has a fixed probability of changing sex in each season; this probability is independent of the state of the population. Thus, the expected proportion of each age-class that is male and female is fixed, and f_i and m_i are treated as constants. In Model 2, sexual transition is dictated by social factors, and the probability that an individual female remains female throughout some season is assumed to be directly proportional to the mean age of the population. This probability is constrained to be less than or equal to 1. Thus, if fishing lowers the mean age of the population, the probability that a female will change sex at a given age increases. Both models are assumed to have the same proportions of males and females in equilibrium in the absence of fishing pressure.

The mortality rate is assumed to be density independent in year-classes 1 through $(\omega - 1)$. Let p_i denote the per capita survival rate of individuals in the ith cohort. Let ν_i and μ_i represent the fertility of females and males of age i, respectively, where fertility describes the rate of reproductive success and is assumed to be proportional to fecundity. Fecundity increases nonlinearly with size, and larger fish contribute disproportionately to the spawning stock; this is accommodated in the ν_i and μ_i values.

Reef fish populations are best modelled as metapopulations of interconnected local populations that communicate through dispersal of pelagic larvae (Sale 1998). This study focuses only on the dynamics of a single local population but explicitly considers its role within the context of the wider metapopulation. The population is both partially open and partially closed. Let ξ represent the external supply rate and a represent the proportion of individuals produced locally that successfully recruit back to their reef of origin.

Production in the local population depends on the number of encounters between males and females, weighted by the fertilities. A constant scaling factor that governs the rate of encounters between individuals from different age-classes is subsumed into the fertility measures. Therefore, P_{t+1}, the production in season $t + 1$, is

$$(1) \qquad P_{t+1} = \left(\sum_{i=1}^{\omega} \nu_i f_i N_{i_t} \right) \left(\sum_{i=1}^{\omega} \mu_i m_i N_{i_t} \right).$$

It could be argued that production should be scaled by some form of marriage function (Caswell 1989), which would relate the density of males and females to the rate of successful reproduction and describe the complex reproductive behaviour of coral trout (Samoilys 1997). However, I know of no studies on serranids that determine what form such a

function would take. Dependence of production on the encounter rate between males and females is one of the simplest relationships that can be assumed.

The supply of larvae to the population in the spawning season at the beginning of year $t + 1$ is

$$(2) \qquad S_{t+1} = aP_{t+1} + \xi.$$

It is assumed that if population regulation occurs, then it occurs in the first year, that it is the per capita mortality rate of individuals in the settling (year 0) cohort that is density dependent, and that the density dependence is compensatory but not overcompensatory. Compensatory density dependence is modelled with a Beverton–Holt type function (Beverton and Holt 1957), with the relationship between supply and recruitment given by

$$(3) \qquad R_{t+1} = \frac{\alpha S_{t+1}}{1 + \beta S_{t+1}}$$

where α describes the survival rate at low densities and α/β determines the saturation limit. Thus, the population models become

$$(4) \qquad N_{1_{t+1}} = R_{t+1} \text{ and } N_{i+1_{t+1}} = p_i N_{i_t} \text{ for } i = 1,...,\omega - 1.$$

The supply–recruitment relationship is rather general, and the dynamics depend entirely on the choice of parameters. If $\beta = 0$, then the mortality rate prior to censusing in the first year is density independent. If β is positive but sufficiently small, then the mortality rate of the settling cohort would be effectively density independent in the majority of years and would be strongly affected by density dependence only in times of anomalously high supply. This may be the case for many local reef fish populations including those of epinepheline serranids (Letourneur et al. 1998).

In Appendix A, how the available data for *P. leopardus* are used in the application of the models is explained. The sensitivity of the conclusions to the model assumptions and the choice of parameter values is reviewed in the Discussion.

Analysis

For brevity, results are presented only for the case where $a \neq 0$ and $\beta \neq 0$. In other words, there is some degree of regular self-recruitment, and year 0 mortality is density dependent. Other cases can be dealt with in a similar fashion. Technical details of the analyses are provided in Appendix B.

In the absence of fishing, critical point solutions of eq. 4 are identical for both models. At equilibrium

$$(5) \qquad \mathbf{N}_{t+1} = \mathbf{N}_t \Rightarrow N_i = \prod_{j=0}^{i-1} p_j N_1 \quad \text{for } i = 2,...,\omega$$

$$P = \left(\sum_{i=1}^{\omega} \nu_i f_i \prod_{j=0}^{i-1} p_j \right) \left(\sum_{i=1}^{\omega} \mu_i m_i \prod_{j=0}^{i-1} p_j \right) N_1^2 = F_0 M_0 N_1^2$$

where

$$(6) \qquad F_0 = \sum_{i=1}^{\omega} \nu_i f_i \prod_{j=0}^{i-1} p_j \text{ and } M_0 = \sum_{i=1}^{\omega} \mu_i m_i \prod_{j=0}^{i-1} p_j$$

570

Can. J. Fish. Aquat. Sci. Vol. 58, 2001

Fig. 1. All figures were produced using the data given in Appendix A. (*a*) Cross-sections of the equilibrium surface plotted against aF_0M_0 for $\xi\beta/\alpha$ = [0, 0.0125, 0.025, 0.05, 0.1, 0.2, 0.4, 0.8, 1.6], given in increasing order of vertical intercept; (*b*) projection of the outlines of the cusp onto the (aF_0M_0, $\xi\beta/\alpha$) plane. The curves separate parameter space into three regions.
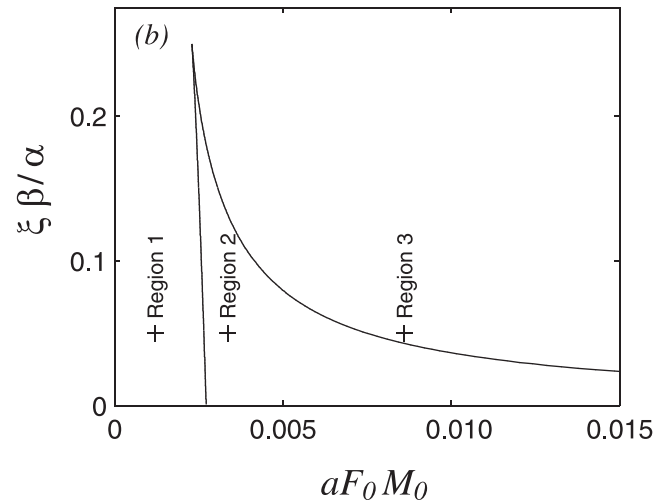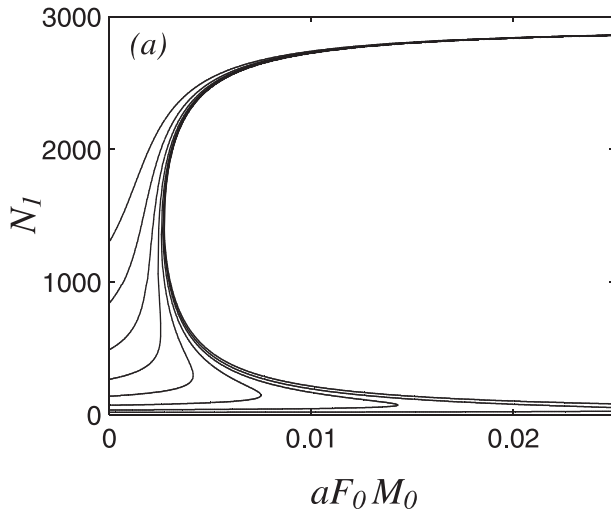
(p_0 = 1 for notational convenience). These definitions adapt the net reproductive number from standard age-structured models (Cushing and Yicang 1994) and measure the expected lifetime reproductive contribution of individuals as females and males.

Critical point solutions for both models are given by roots of

(7) $g(N_1) = a\beta F_0 M_0 N_1^3 - a\alpha F_0 M_0 N_1^2 + (1 + \beta\xi)N_1 - \alpha\xi = 0$

(see Appendix B). This cubic has one or three positive roots. When fishing pressure is introduced, the f_i and m_i terms differ between the two models, and consequently, the F_0 and M_0 terms also differ. However, the cubic is unaffected by the additional nonlinearity in Model 2 because the mean age of the population is independent of the population size at equilibrium. Thus, eq. 7 still determines critical point solutions for Model 2.

The population dynamics for both models are characterised by a cusp catastrophe, in which the equilibrium surface is folded over on itself in parameter space (Drazin 1992). Such dynamics often arise when considering the interaction between nonlinear production terms with compensatory density dependence (Cushing 1996). Cross-sections of the equilibrium surface showing the fold are given in Fig. 1*a*. Double roots of the cubic determine the outlines of the fold, and the curves corresponding to such roots separate parameter space into three distinct regions (Fig. 1*b*).

The concept of source and sink dynamics (Thomas and Kunin 1999) proves helpful when distinguishing among regions of parameter space. Several definitions of source and sink dynamics are employed in the literature. Here, a source population is defined to be one in which the local rate of successful self-recruitment exceeds the local death rate; the inequality is reversed in a sink population. A source population is self-sustaining, but a sink population depends on external supply for its persistence.

Region 1 in Fig. 1*b* corresponds to dynamics possessing a single stable critical point solution that represents a sink population. Region 2 is characterised by the existence of three critical point solutions: two stable attractors separated by an unstable threshold. The lower stable critical point rep-

resents a sink state, and the larger represents a source state. Region 3 has a single stable equilibrium that represents a source state.

Local population dynamics appear to be more sensitive to the self-recruitment rate *a* than to the external supply rate ξ. Variations in *a* correspond to horizontal movements through parameter space in Fig. 1*b*, which can shift the population between regions that have markedly different qualitative dynamics.

Monte Carlo simulations

Rates of arrival of larvae at sites suitable for settlement are extremely variable. Monte Carlo simulations were designed to examine how the underlying deterministic dynamics of a local population might interact with this variability. Details regarding the construction of the simulations are given in Appendix B.

While critical point solutions are identical for both models in the absence of fishing, transient dynamics differ. However, the differences prove slight, and results from both models are almost identical for the same set of simulated *a* and ξ for the unfished case. What minor differences do arise result from fluctuations in recruitment that drive fluctuations in the mean age of the population in Model 2. These fluctuations in mean age feed back into local productivity via fluctuations in the sex ratio. However, the sex ratio never shifts far from that observed in the data to which both models are fitted.

Sink populations in Region 1 fluctuate around the single stable attractor for both models (Fig. 2*a*). The number of recruits joining the first year-class displays nearly perfect correlation with external supply (correlation coefficient $\rho = 1.00$ for the trajectory shown), and distortion of supply fluctuations due to density dependence is negligible.

Source populations in Region 3 also fluctuate around a single, globally stable attractor. Fluctuations are asymmetric, and perturbations that decrease population size are larger than those that increase population size (Fig. 2*b*). This is the opposite pattern to that displayed by both the *a* and ξ distributions (small values in most years with sporadic good years when the values obtained are much larger). Numerical ex-

Fig. 2. Simulated population abundances (summed across all 14 cohorts) for Models 1 and 2. The thick broken line is mean abundance from 40 simulations for Model 1 and thin broken lines represent ±2 SD. A single realisation for both models is graphed with solid lines, and Model 1 is represented by the thicker of these lines. (*a*) Sink population data from Region 1 when variance is low (CV = $1/\sqrt{3}$ for *a* and ξ); (*b*) source population data from Region 3 when variance is low (CV = $1/\sqrt{3}$ for *a* and ξ); (*c*) population having two stable equilibria when variance is high (CV = 4 for *a* and ξ).
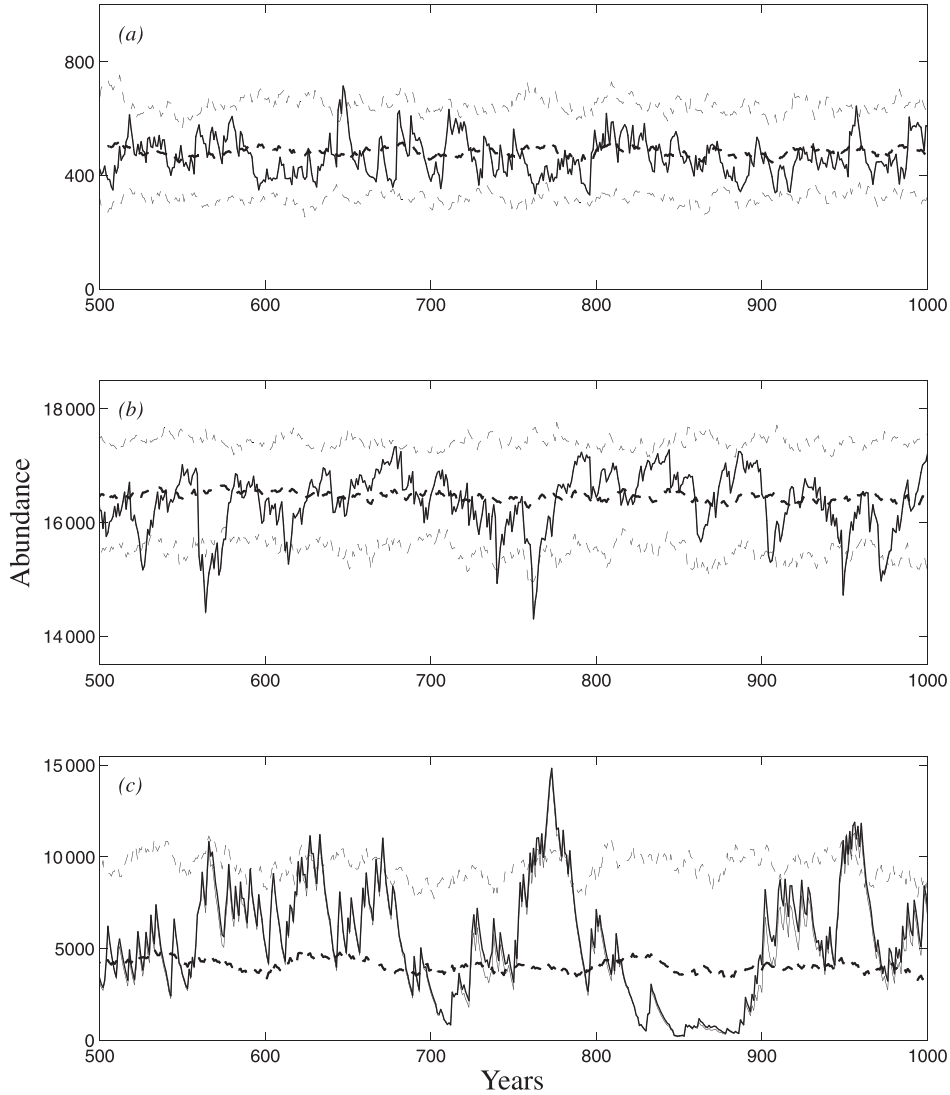
periments in which one variable is held constant indicate that the fluctuations in abundance are primarily driven by variations in self-recruitment rate *a*.

In the interior of Region 2, the dynamics show behaviour similar to that for the deterministic cusp when variance in *a* and ξ is low. The population converges on one of the two stable attractors (source or sink), and which is approached depends on the initial conditions. As variance is increased, fluctuations in *a* cause the population to shift sporadically between source and sink status (Fig. 2*c*).

More complex behaviour can arise in the region around the cusp curves themselves because of an interaction between recruitment fluctuations and the bifurcation behaviour of the models. For parameter values around the lower cusp curve, low initial population sizes lead to sink dynamics, but the population fluctuates around a region where the other two equilibria appear intermittently for larger initial population sizes. Variance in population size is greatly increased in

this region, and the population fluctuates widely in response to fluctuations in *a* (Fig. 3). Eventually, a string of poor recruitment years leads to the sudden collapse of the population to permanent sink status. Similar dynamics arise around the upper cusp curve.

Effects of harvesting

Having described the different population dynamics, we can now examine the effects of fishing. The catch-per-unit-effort hypothesis (Hilborn and Walters 1992) is adopted and the effort level is denoted by *E*. Vector $\mathbf{q} = (q_1,...,q_\omega)$ defines the catchability coefficients for each cohort. It is assumed that individuals do not become susceptible to capture until after the census time at the end of their first year and that fishing occurs after reproduction. The population dynamics under harvest are given by

572

Can. J. Fish. Aquat. Sci. Vol. 58, 2001

Fig. 3. Simulated population abundances (summed across all 14 cohorts) for Models 1 and 2 near the lower bifurcation with low variance (CV $=1/\sqrt{3}$ for a and ξ). A single realisation for both models is graphed with solid lines, and Model 1 is represented by the thicker of these lines. At $t = [1000, 1500, 2000]$, the mean abundance ± 2 SD is shown for Model 1 for the subset of 60 simulations initialised in a source state that have not yet collapsed to sink status: $n = [48, 42, 36]$, respectively. Collapses to sink status followed a string of poor self-recruitment years. After collapse, all populations remained in the sink state for the remainder of the simulation (5000 years).
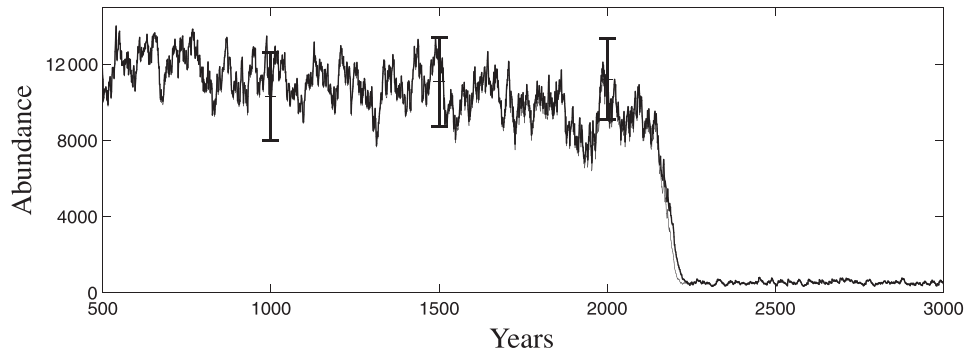
$$(8) \qquad N_{1_{t+1}} = R_{t+1} \text{ and } N_{i+1_{t+1}} = (p_i - q_i E)N_{i_t}$$
$$\text{for } i = 1,...,\omega - 1.$$

Both models have the same structure as eq. 4. Fishing mortality reduces the effective p_i values and thus also reduces the effective F_0M_0 value. This causes a shift to the left through parameter space that is parallel to the aF_0M_0 axis in Fig. 1b, the magnitude of which differs for the two models. This change in parameter values corresponds to a shift from source towards sink status. An increase in fishing mortality can take a population from a regime characterised by a single stable state through a region containing two stable states in which population size varies widely in response to varying supply rates. In summary, an increase in fishing effort in either model could result in a decrease in population abundance, a shift from source to sink status, an increase in variability in population size caused by fluctuations in supply rates, and the possibility of sudden, unpredictable collapse of seemingly stable stocks at some future time. An intensification of fishing need only result in the first of these four conclusions, and which ones are realised will depend on the natural state of the population and the extent of fishing mortality.

Gear selectivity

To assess the vulnerability of the population to selective gear, one must examine how F_0M_0 decreases when fishing mortality is introduced in each model. Cases where the fishery catches the same yield in overall biomass are compared. Greater effort is required to catch a fixed yield when relying on a highly selective strategy than is required when relying on a nondiscriminatory strategy. If the required yield is too large, then highly selective strategies will not be feasible. The optimal feasible selectivity strategy is defined as the one that causes the least reduction in F_0M_0 and hence incurs the least risk of overfishing while providing some specified yield.

Details concerning how the F_0M_0 values were computed for each model under harvest are given in Appendix A. Let (i, j) represent an exploitation strategy where the fishery targets the ith through jth cohorts where $i \in [1,...,\omega]$ and $j \in [i,...,\omega]$. Figure 4 illustrates the effect on F_0M_0 of harvesting an annual catch equivalent to 3.3% of virgin biomass when using different strategies. Each circle represents a feasible exploitation

strategy, and the solid circle in the back corner represents the optimal strategy. The optimal strategy for both models is one that targets only the oldest fish in the population.

The sensitivity of the optimal selectivity strategy to the assumed growth schedule, the mean age of sexual transition, the survivorship rate, and the level of harvesting for both models was explored. A single parameter was varied each time, and the remaining parameters were fixed at their specified values. For a large region of parameter space centred upon the data for coral trout, the optimal strategy for both models lies in the back corner of the set of allowable strategies and involves targeting only older age-classes. An exception to this occurs for low survivorship probabilities. When the survivorship probabilities are particularly low, then the majority of the settling cohort are lost to natural mortality in the first few years of life. It can be optimal in this situation to harvest only younger individuals that would otherwise be lost to the fishery.

Fishing alters the population's age and sex structure for both models. Figure 5 compares scenarios where there is no fishing, where the gear is not selective and an annual catch equivalent to 2.75% of virgin biomass is harvested, and where the gear selectively targets the oldest (10+) cohorts and the same overall biomass is caught. Fishing strategies that target the oldest cohorts cause less disturbance to the natural sex structure of the population than less discriminatory strategies. Size-selective fishing also results in a greater overall mean age and a greater mean age of females than less selective fishing practices.

The most substantial differences between the two models arise in the consequences of fishing mortality for population structure. The number of individuals surviving to reach older age-classes decreases when fishing mortality is imposed. In Model 1, this has a disproportionate effect on the male life stages. Therefore, the sex ratio becomes female biased (Figs. 5b and 5d). In Model 2, decreased survivorship lowers the mean age of the population and triggers younger sexual transition. The number and size of females in the population decrease as a result, and the sex ratio becomes male biased because the population overcompensates for impacts to its sex ratio (Figs. 5c and 5e). For both models, changes in population structure are most pronounced for indiscriminate fishing practices.

Fig. 4. Comparison of selectivity strategies when a fixed harvest is taken (equivalent to 3.3% of virgin biomass) for (*a*) Model 1 and (*b*) Model 2. Equal catchability of targeted cohorts is assumed. Circle (i, j) represents a feasible strategy that targets cohorts i through j, and the solid circle represents the optimal selectivity pattern.
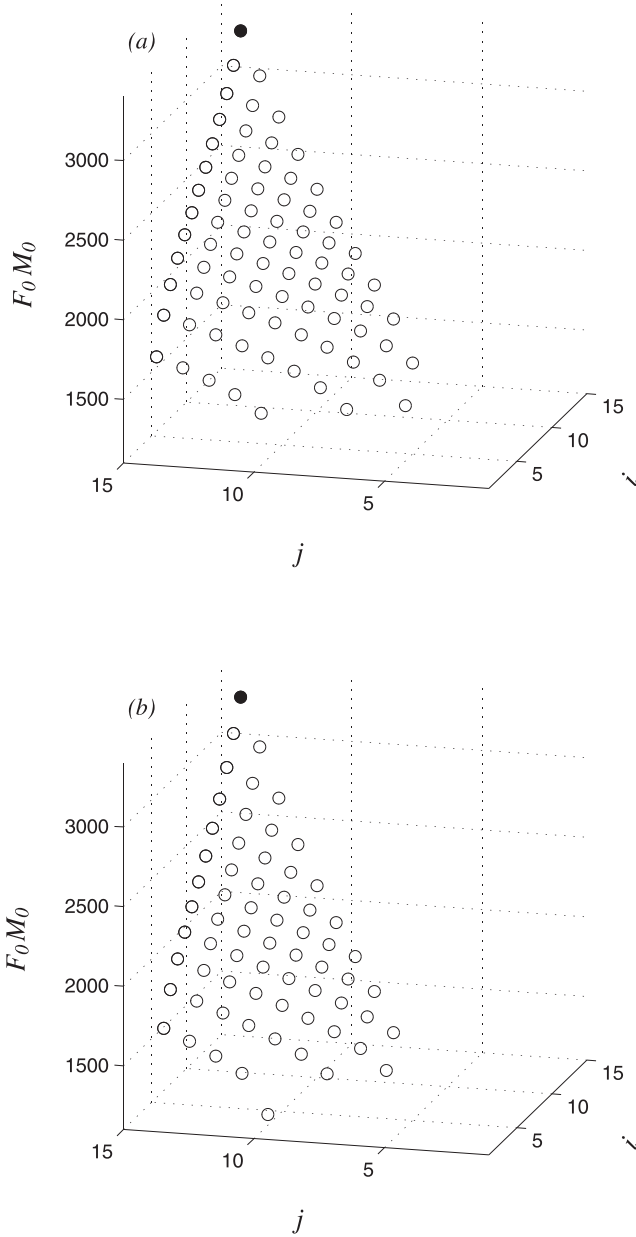
Discussion

The deterministic models capture the essential dynamics of the situations under examination: those of partially open populations of protogynous hermaphrodites in which sexual transition responds to either endogenous or exogenous mechanisms (Models 1 and 2, respectively) and that are subjected to harvesting pressure. The resulting dynamics are characterised by a cusp catastrophe, one of the best understood of nonlinear phenomena (Drazin 1992) with well-studied implications for the management of natural systems

(May 1977). Monte Carlo simulations reveal that the deterministic models perform well in regions of parameter space where they would be expected to be robust to perturbations, i.e., away from the bifurcations. Results from the deterministic analyses are not directly analogous to those from the stochastic simulations in the region around the bifurcations or when the variance in parameter values is high. Further modelling work examining more complex reproductive dynamics and more sophisticated mechanisms governing sexual transition would be worthwhile. The modelling framework presented here would provide a useful starting point for such analyses and for studies examining the effects of harvesting on other hermaphrodites.

Substantial uncertainty surrounds many of the processes involved, and one should consider any sensitivity to the assumptions made and the particular parameter values employed. The assumption regarding the density-dependent mortality in the first year of life can be relaxed and a similar analysis applies, although a source population grows without bound. If the mortality rate were characterised by over-compensatory density dependence or if other demographic rates were density dependent, then different dynamics could result.

The assumption that reproductive success is proportional to the number of encounters between males and females is one of the simplest about reproduction that could have been employed. It would be interesting to incorporate a more sophisticated marriage function (Caswell 1989) that represents the complex reproductive behaviour of coral trout (Samoilys 1997). However, provided there is some dependence of the per capita reproductive success of females on the number of males, then the population dynamics will be characterised by a threshold effect with multiple equilibria and similar conclusions will apply. Bannerot et al. (1987) used simulations to compare the vulnerability of protogynous hermaphrodites and gonochoristic species to overfishing under different assumptions about reproduction and concluded that hermaphrodites would be the more vulnerable as the likelihood of sperm limitation increased.

Uncertainty remains about many of the parameter values used such as the age-specific mortality rates and catchabilities, the rate of fertilisation success, and the rate of successful self-recruitment. This uncertainty can be accommodated because these processes are summarised by a single statistic, aF_0M_0. The population dynamics were examined for all possible values of this quantity. The conclusions regarding size-selective fishing proved robust when exploring a large region of parameter space centred on the data for coral trout.

Effects of harvesting

A general trend that appears in these and many other models is that fishing results in a shift from source status towards sink status. If a population were to lie in Region 3 when unexploited and external recruitment had not failed, then a shift to sink status could be reversed and the population would recover were fishing to cease. However, if a population were in Region 2 when unexploited or external recruitment failed, then a shift to sink status could be irrevocable. As indicated by the stochastic analyses, shifts to sink status can be sudden and dramatic, even for a fishery that had been sustainable for many years. This tends to occur

Fig. 5. Effect of different fishing strategies on population structure. Equal catchability of targeted cohorts is assumed. Shaded bars represent males and solid bars females. (*a*) Natural state of the source population; same for both models. Sex ratio of males to females m:f = 1:1.70, mean age $\overline{\mathbf{W}}^* = 5.26$, mean female age $\overline{\mathbf{W}}_f^* = 4.25$, and $F_0M_0 = 3274$. (*b* and *c*) New equilibrial population structure reached when annually removing 2.75% of the total virgin biomass through nonselective harvesting of all age-classes 1,..., ω for (*b*) Model 1 (m:f = 1:2.13, $\overline{\mathbf{W}} = 4.67$, $\overline{\mathbf{W}}_f = 4.05$, $F_0M_0 = 1816$) and (*c*) Model 2 (m:f = 1:0.72, $\overline{\mathbf{W}} = 4.62$, $\overline{\mathbf{W}}_f = 3.58$, $F_0M_0 = 1511$). (*d* and *e*) New equilibrial population structure reached when removing the same amount of biomass annually through selective harvesting targeting of cohorts 10,..., ω for (*d*) Model 1 (m:f = 1:1.92, $\overline{\mathbf{W}} = 4.98$, $\overline{\mathbf{W}}_f = 4.23$, $F_0M_0 = 2840$) and (*e*) Model 2 (m:f = 1:1.09, $\overline{\mathbf{W}} = 4.97$, $\overline{\mathbf{W}}_f = 4.00$, $F_0M_0 = 2766$).
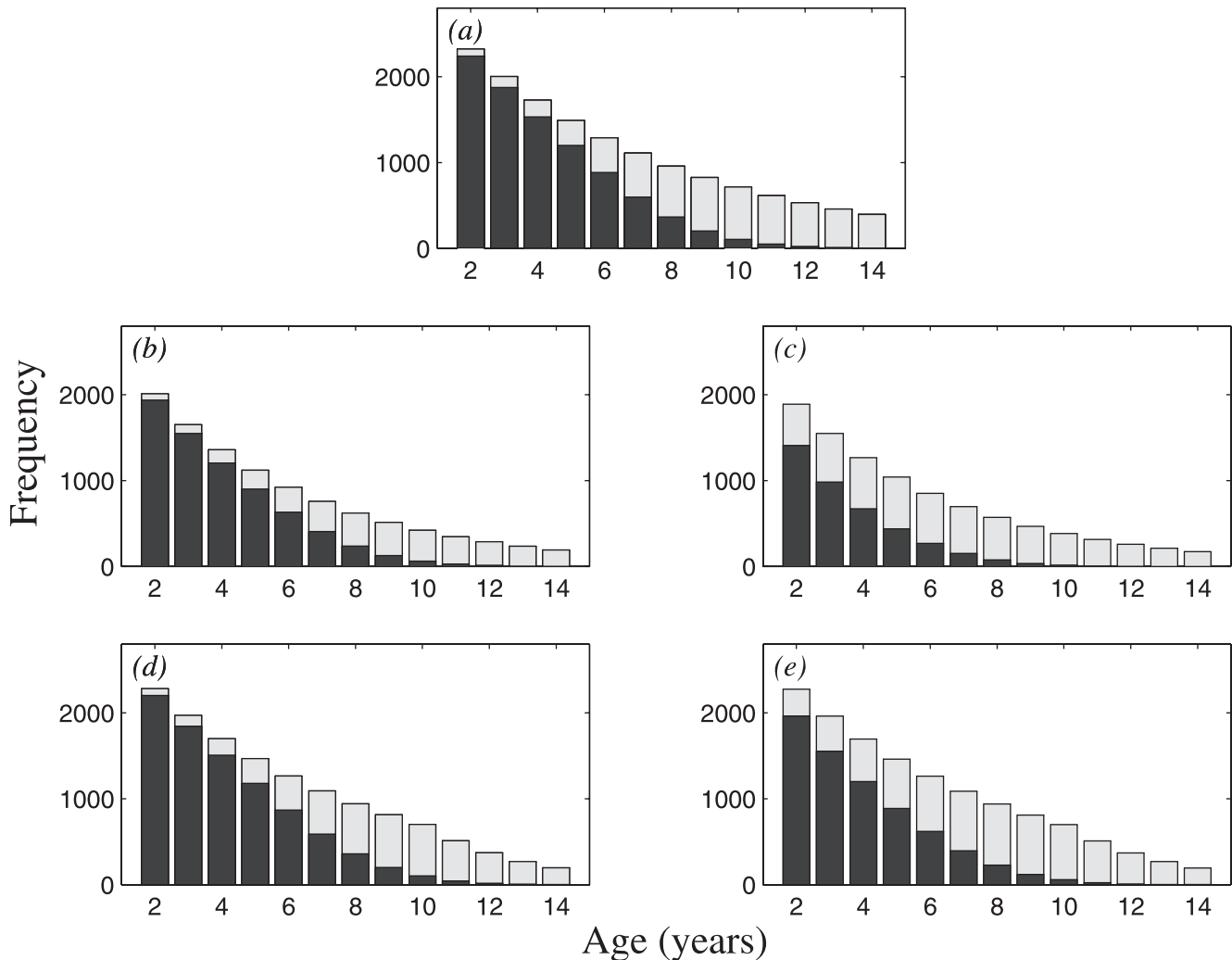
when the population is subjected to the cumulative stress of fishing and a run of poor recruitment years. A shift from source to sink status results in a local population becoming entirely dependent on external supply. If that supply comes from outside the jurisdictional boundaries of the management agency, this shift results in the effective loss of sovereignty over the stock because persistence is contingent on events elsewhere.

The collapse of source populations can have metapopulation-wide consequences. Persistence of metapopulations, which could comprise entire stocks in large geographic regions, is contingent on the persistence of their local source populations or subregions. The fewer of these sources that remain, the less resilient a metapopulation is to catastrophic disturbance and the greater the risk of total regional stock collapse.

Gear selectivity

In both models, fishing alters both the sex ratio and the age structure of the population. Selectively targeting only older individuals results in a greater mean age in the population and has less effect on the sex ratio than less selective harvesting. The change in aF_0M_0 that corresponds to an increase in fishing effort is lowest when only older age-classes are targeted, and hence, selective fishing can minimise the risk of overfishing while supplying the same overall catch.

On the Great Barrier Reef, the minimum legal size for catching coral trout is 38 cm, which corresponds to an age of from 2 to 5 years. The precise mechanisms governing sexual transition in this species are unknown and will be difficult to detect (Ferreira and Russ 1995). The models suggest that a larger minimum size limit could be more efficient for

both transition mechanisms. Thus, more efficient management practices could be implemented now without requiring precise knowledge of the sex-changing mechanisms. However, further research into the reproductive behaviour of coral trout would improve our understanding of where any thresholds between source and sink status might lie.

Acknowledgements

References

Bannerot, S., Fox, W.W., Jr., and Powers, J.E. 1987. Reproductive strategies and the management of snappers and groupers in the Gulf of Mexico and Caribbean. *In* Tropical snappers and groupers: biology and fisheries management. *Edited by* J.J. Polovina and S. Ralston. Westview, Boulder, Co. pp. 561–603.

Beverton, R.J.H., and Holt, S.J. 1957. On the dynamics of exploited fish populations. Ministry of Agriculture, Fisheries and Food, London, U.K.

Buxton, C.D. 1993. Life-history changes in exploited reef fishes on the east coast of South Africa. Environ. Biol. Fishes, **36**: 47–63.

Caswell, H. 1989. Matrix population models. Sinauer Associates, Sunderland, Mass.

Cushing, J.M. 1996. Nonlinear matrix equations and population dynamics. *In* Structured-population models in marine, terrestrial, and freshwater systems. *Edited by* S. Tuljapurkar and H. Caswell. Chapman and Hall, New York. pp. 205–243.

Cushing, J.M., and Yicang, Z. 1994. The net reproductive value and stability in matrix population models. Nat. Resour. Model. **8**: 297–333.

Doherty, P.J., Fowler, A.J., Samoilys, M.A., and Harris, D.A. 1994. Monitoring the replenishment of coral trout (Pisces: Serranidae) populations. Bull. Mar. Sci. **54**: 343–355.

Drazin, P.G. 1992. Nonlinear systems. Cambridge University Press, Cambridge, U.K.

Ferreira, B.P. 1995. Reproduction of the common coral trout *Plectropomus leopardus* (Serranidae: Epinepheline) from the Central and Northern Great Barrier Reef, Australia. Bull. Mar. Sci. **56**: 653–669.

Ferreira, B.P., and Russ, G.R. 1994. Age validation and estimation of growth rate of the coral trout, *Plectropomus leopardus* (Lacepede 1802), from Lizard Island, Northern Great Barrier Reef. Fish. Bull. U.S. **92**: 46–57.

Ferreira, B.P., and Russ, G.R. 1995. Population structure of the leopard coralgrouper, *Plectropomus leopardus*, on fished and unfished reefs off Townsville, Central Great Barrier Reef, Australia. Fish. Bull. U.S. **93**: 629–642.

Hilborn, R., and Walters, C.J. 1992. Quantitative fisheries stock assessment: choice, dynamics and uncertainty. Chapman and Hall, New York.

Letourneur, Y., Chabanet, P., Vigliola, L., and Harmelin-Vivien, M. 1998. Mass settlement and post-settlement mortality of *Epinephelus merra* (Pisces: Serranidae) on Reunion coral reefs. J. Mar. Biol. Assoc. U.K. **78**: 307–319.

May, R.M. 1977. Thresholds and breakpoints in ecosystems with a multiplicity of stable states. Nature (Lond.), **269**: 471–477.

Ross, R.M. 1990. The evolution of sex-change mechanisms in fishes. Environ. Biol. Fishes, **29**: 81–93.

Russ, G.R. 1991. Coral reef fisheries: effects and yields. *In* The ecology of fishes on coral reefs. *Edited by* P.F. Sale. Academic Press, San Diego, Calif. pp. 601–635.

Sale, P.F. 1998. Appropriate spatial scales for studies of reef-fish ecology. Aust. J. Ecol. **23**: 202–208.

Samoilys, M.A. 1997. Periodicity of spawning aggregations of coral trout *Plectropomus leopardus* (Pisces: Serranidae) on the northern Great Barrier Reef. Mar. Ecol. Prog. Ser. **160**: 149–159.

Samoilys, M.A., and Squire, L.C. 1994. Preliminary observations on the spawning behaviour of coral trout, *Plectropomus leopardus* (Pisces: Serranidae), on the Great Barrier Reef. Bull. Mar. Sci. **54**: 332–342.

Shapiro, D.Y. 1989. Sex change as an alternative life-history style. *In* Alternative life-history styles of animals. *Edited by* M.N. Bruton. Kluwer Academic Publishers, Dordrecht, The Netherlands. pp. 177–195.

Thomas, C.D., and Kunin, W.E. 1999. The spatial structure of populations. J. Anim. Ecol. **68**: 647–657.

Thompson, R., and Munro, J.L. 1983. The biology, ecology and bionomics of the hinds and groupers. *In* Caribbean coral reef fishery resources. *Edited by* J.L. Munro. ICLARM, Manila, Philippines.

Thresher, R.E. 1984. Reproduction in reef fishes. T.F.H. Publications, Neptune City, N.J.

Appendix A

The maximum age for *P. leopardus* was taken to be $\omega = 14$ years (Ferreira and Russ 1994). The age of first reproduction is set at 2 years (Ferreira 1995). The expected proportions of males and females in each cohort in the absence of fishing are taken from Ferreira's (1995) Lizard Island data. For convenience, transitional individuals were classified as male. A least squares regression was used to fit these data to a curve of the form

$$(A1) \quad \frac{1 - \tanh(c_1(t - c_2))}{2}$$

($c_1 = 0.32$, $c_2 = 7.24$) and the fitted data were employed in the model applications; c_2 determines the mean time of sexual transition and c_1 determines the dispersion about this mean. Age-specific probabilities of remaining female for a given age in the absence of fishing can be computed:

$$(A2) \quad T_1 = f_1 \text{ and } T_i = f_i/f_{i-1} \quad \text{for } i = 2,...,\omega.$$

Ferreira and Russ (1994) approximated the growth rate of *P. leopardus* in the Central Great Barrier Reef with Schnute's (1981) generic equation. For the specific data, Schnute's formula was found to be equivalent to the von Bertalanffy growth curve for length at time t:

$$(A3) \quad L(t) = L_\infty(1 - e^{-K(t-t_o)})$$

where $L_\infty = 52.2$ cm is the asymptotic length, $K = 0.354$ is the growth coefficient, and $t_0 = -0.766$ is the hypothetical age at which length is zero. From this length-based approximation, an equivalent expression can be obtained for the weight of individuals of a given age.

Per capita survivorship coefficients were taken as constant throughout the life cycle. The mortality rate is taken from the

catch-per-unit-effort data of Russ et al. (1998) (only available for years 6 through 9): $p_i = 0.863$ for $i = 1,...,\omega - 1$.

Sadovy (1996) reviewed the available data on fecundity and gave an approximation for the female fecundity $\tilde{F}$ of groupers as a function of body length L:

(A4) $\tilde{F} = 0.0129L^{3.03}$.

For want of alternative data, the fecundity of males is assumed proportional to the fecundity of females of the same age. The results are not sensitive to the constant of proportionality chosen.

Estimates of parameters α and β are not available. To produce the figures, the probability of individuals surviving settlement when settling in low densities was taken as $\alpha = 0.5$. Parameter β was chosen so that source population size was 17 500, which is roughly comparable with estimated population sizes at Lizard Island (Zeller and Russ 2000). Source population size was chosen because there is evidence from other species to suggest a significant degree of self-recruitment to Lizard Island (Jones et al. 1999).

Good data are not available for the rate of supply to reefs from external populations or for the proportion of locally produced propagules that survive to successfully recruit back to their reef of origin. However, the regions of parameter space in which these values must lie can be deduced from what is known of the ecology of coral trout and from dimensional analyses. The dynamics for the full range of plausible parameter values are examined in the deterministic model and simulations. In the section on the effect of harvesting, $\xi = \alpha/(20\beta)$ and $a = 2.63 \times 10^{-6}$ (corresponding to 35% larval mortality rate per day for a 25-day pelagic larval stage, with one in every eight surviving larvae returning to their reef of origin).

For the unfished case, F_0M_0 is directly proportional to the equivalent quantity when fecundities are used in place of fertilities in eq. 6. The constant of proportionality is chosen so that the parameters correspond to the right-hand cross in Fig. 1b.

When a fixed yield in overall biomass is to be harvested, the required effort can be computed under the assumption of equal catchability of targeted cohorts and from the equivalent expression to eq. A3 for weight. Therefore, new survivorship coefficients can be obtained, $\hat{p} = p - qE$, and F_0M_0 values under harvest obtained for Model 1.

New $\hat{f}_i$ and $\hat{m}_i$ values must also be computed for Model 2 because harvesting changes the mean age of the population. Let $\overline{\mathbf{W}}$ and $\overline{\mathbf{W}}^*$ denote the mean ages of the harvested and unharvested populations, respectively. In equilibrium,

(A5) $\overline{\mathbf{W}} = \dfrac{\sum\limits_{i=1}^{\omega} i \prod\limits_{j=0}^{i-1} \hat{p}_j}{\sum\limits_{i=1}^{\omega} \prod\limits_{j=0}^{i-1} \hat{p}_j}$

A similar expression holds for $\overline{\mathbf{W}}^*$. When fishing pressure is applied in Model 2, the probabilities of remaining female at some age become

(A6) $T_1 = f_1 \overline{\mathbf{W}}/\overline{\mathbf{W}}^*$ and $T_i = (f_i \overline{\mathbf{W}})/(f_{i-1}\mathbf{W}^*)$

for $i = 2,...,\omega$.

Then

(A7) $\hat{f}_i = f_i(\overline{\mathbf{W}}/\overline{\mathbf{W}}^*)^i$ for $i = 1,...,\omega$

with the constraint imposed that $\hat{f}_i$ must be less than or equal to 1. Hence, the new $\hat{m}_i$ values, and consequently the new F_0M_0 values, can be obtained.

Appendix A references

Ferreira, B.P. 1995. Reproduction of the common coral trout *Plectropomus leopardus* (Serranidae: Epinepheline) from the Central and Northern Great Barrier Reef, Australia. Bull. Mar. Sci. **56**: 653–669.

Ferreira, B.P., and Russ, G.R. 1994. Age validation and estimation of growth rate of the coral trout, *Plectropomus leopardus* (Lacepede 1802), from Lizard Island, Northern Great Barrier Reef. Fish. Bull. U.S. **92**: 46–57.

Jones, G.P., Milicich, M.J., Emslie, M.J., and Lunow, C. 1999. Self-recruitment in a coral reef fish population. Nature (Lond.), **402**: 802–804.

Russ, G.R., Lou, D.C., Higgs, J.B., and Ferreira, B.P. 1998. Mortality rate of a cohort of the coral trout, *Plectropomus leopardus*, in zones of the Great Barrier Reef Marine Park closed to fishing. Mar. Freshwater Res. **49**: 507–511.

Sadovy, Y.J. 1996. Reproduction of reef fishery species. *In* Reef fisheries. *Edited by* N.V.C. Polunin and C.M. Roberts. Chapman and Hall, London, U.K. pp. 15–59.

Schnute, J. 1981. A versatile growth model with statistically stable parameters. Can. J. Fish. Aquat. Sci. **38**: 1128–1140.

Zeller, D.C., and Russ, G.R. 2000. Population estimates and size structure of *Plectropomus leopardus* (Pisces: Serranidae) in relation to no-fishing zones: mark–release–resighting and underwater visual census. Mar. Freshwater Res. **51**: 221–228.

Appendix B

At equilibrium, solutions of eq. 4 for both models solve

(B1) $N_1 = \dfrac{\alpha(aF_0M_0N_1^2 + \xi)}{1 + \beta(aF_0M_0N_1^2 + \xi)}$

which gives eq. 7 on rearranging.

The cusp curves in Fig. 1b describe parameter sets for which eq. 7 has double roots. Let

(B2) $N_1 = Q + \dfrac{\alpha}{3\beta} \Rightarrow 0 = Q^3 - uQ + v$

where

$u = \dfrac{\alpha^2}{3\beta^2} - \dfrac{1 + \beta\xi}{a\beta F_0M_0}$

and

$v = \dfrac{-2\alpha^3}{27\beta^3} + \dfrac{\alpha(1 - 2\xi\beta)}{3a\beta^2 F_0M_0}$.

Turning points of the cubic solve

(B3) $0 = 3Q^2 - u \Rightarrow Q = \sqrt{u/3}$.

Double roots are found by solving eqs. B2 and B3 simultaneously to give

(B4) $v^2 = 4u^3 / 27$.

Substituting for u and v in eq. B4 and rearranging gives

(B5) $0 = (aF_0M_0)^2 + \dfrac{8\beta^2\xi^2 - 20\beta\,\xi - 1}{4\alpha^2\xi}(aF_0M_0) + \dfrac{\beta(1+\beta\xi)^3}{\alpha^4\xi}$.

The projection of the cusp outline onto the $(aF_0M_0, \alpha\xi/\beta)$ plane shown in Fig. 1b was drawn by solving eq. B5 as a quadratic in aF_0M_0.

Stability properties of each equilibrium are governed by the magnitude of the dominant eigenvalue(s) of the Jacobian. The magnitude of the dominant eigenvalue must be less than 1 for a critical point to be stable. The Jacobian for Model 1 has a particular, well-studied form. If G_i denotes the growth function for the ith cohort, then:

(B6) $\quad \dfrac{\partial G_i}{\partial N_j} = p_j$ if $j = i-1$ and $\dfrac{\partial G_i}{\partial N_j} = 0$ otherwise.

For the first age-class:

(B7) $\quad \dfrac{\partial R}{\partial N_j} = \dfrac{dR}{dP}\dfrac{\partial P}{\partial N_j} = \dfrac{dR}{dP}\left(\nu_j f_j \sum_{i=1}^{\omega}\mu_i m_i N_i + \mu_j m_j \sum_{i=1}^{\omega}\nu_i f_i N_i \right)$

Let R' denote the derivative of R with respect to P, $F = \Sigma_{i=1}^{\omega}\nu_i f_i N_i$, $M = \Sigma_{i=1}^{\omega}\mu_i m_i N_i$, and $\mathcal{T}_j = \nu_j f_j M + \mu_j m_j F$. The Jacobian is of the form

(B8) $\begin{pmatrix} \mathcal{T}_1 R' & \mathcal{T}_2 R' & \cdots & & \cdots & \mathcal{T}_\omega R' \\ p_1 & 0 & \cdots & & \cdots & 0 \\ 0 & p_2 & \ddots & & & \vdots \\ \vdots & \ddots & \ddots & & & \vdots \\ \vdots & & \ddots & \ddots & \ddots & \vdots \\ 0 & \cdots & & 0 & p_{\omega-1} & 0 \end{pmatrix}$.

A compensatory density dependence is considered, the supply–recruitment relationship is not backwards bending, and R' is always positive. Therefore, the Jacobian is nonnegative and takes the form of the familiar Leslie matrix. Nonnegativity of a matrix implies that its dominant eigenvalue is nonnegative (Caswell 1989).

The dominant eigenvalue of a Leslie matrix is less than 1 if and only if the net reproductive number for the population is less than 1 (Cushing and Yicang 1994). Therefore, the dominant eigenvalue λ of the Jacobian matrix for this model is less than 1 if and only if

(B9) $1 > \sum_{i=1}^{\omega} \dfrac{\partial R}{\partial N_i} \prod_{j=0}^{i-1} p_j = \left(\left(\sum_{i=1}^{\omega}\nu_i f_i \prod_{j=0}^{i-1}p_j \right) M \right.$

$\left. + \left(\sum_{i=1}^{\omega}\mu_i m_i \prod_{j=0}^{i-1}p_j \right) F \right) R'$

$\Leftrightarrow 1 > 2F_0M_0N_1R'$.

The stability analysis for Model 1 is completed by a graphical argument examining $R'(P)$ at each of the equilibria. Plotting $R(P)$ and $N_1 = (P/(F_0M_0))^{1/2}$ establishes that

Fig. B1. Graphical argument establishing stability of equilibria in eq. B9 for Region 2 in Fig. 1b. The broken curve $N_1(P)$ intersects the solid curve $R(P)$ from below for the first and third intersections and from above for the second intersection.
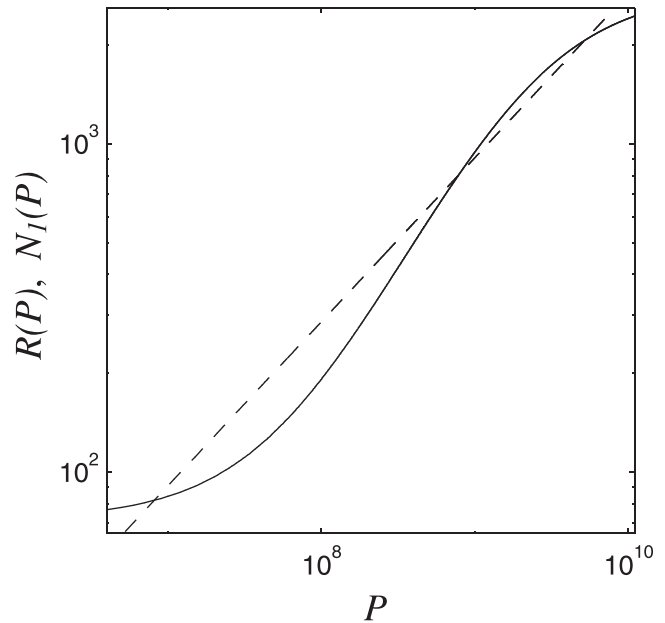
(B10) $\quad R' < \dfrac{1}{2(F_0M_0P)^{1/2}} = \dfrac{1}{2F_0M_0N_1}$

at a single equilibrium or at the smallest and largest equilibria when there are three intersections of these curves (Fig. B1). This implies stability. The required inequality is reversed for the middle equilibrium when there are three intersection points, which implies instability. A stability analysis for Model 2 would be more involved and is not included here. The close match of the two sets of simulations for all parameter values indicates that the stability properties are essentially unchanged (Figs. 2 and 3).

In the simulations, a and ξ were treated as independent random variables in each year, and no serial correlation was considered. Other parameters were fixed at the values described in Appendix A. Parameter a was sampled from an asymmetric β distribution so that $a \in [0,1]$, and in most years, a was extremely small. Parameter ξ was drawn from a lognormal distribution. Simulations for both Models 1 and 2 were performed using each a and ξ data set. Simulations were repeated with one variable held constant and the other allowed to fluctuate according to its probabilistic distribution to assess the relative contributions to observed dynamics from fluctuations in a and ξ. Mean values for the two distributions were assigned from a uniform grid that covered the region of parameter space shown in Fig. 1. Coefficients of variation for both a and ξ distributions were kept equal for consistency. For low-variance simulations, CV $= 1/\sqrt{3}$, and for high-variance simulations, CV $= 4$. Forty simulations were performed for each assigned mean value, and each ran for 1000 years. Sample paths are shown in Fig. 2. For each run, the population was initialised in its equilibrium age distribution, and initial values for N_1 were randomly assigned from a uniform distribution. The first 500 years of data were

discarded to allow the dynamics to equilibrate. Around the bifurcations, simulations were repeated over a finer grid of mean a and ξ values. In this region of parameter space, 60 simulations were performed for each mean value, and each ran for 5000 years. Sample paths for these longer simulations are shown in Fig. 3.

Appendix B references

Caswell, H. 1989. Matrix population models. Sinauer Associates, Sunderland, Mass.

Cushing, J.M., and Yicang, Z. 1994. The net reproductive value and stability in matrix population models. Nat. Resour. Model. **8**: 297–333.